Supporting Information

Nitrogen-Coordinated Cobalt Embedded in Hollow Carbon Polyhedron for Superior Catalytic Oxidation of Organic Contaminants with Peroxymonosulfate

Yaowen Gao[a], Yue Zhu[a], Zhenhuan Chen[a], Chun Hu[a,b,*]

[a]Institute of Environmental Research at Greater Bay, Key Laboratory for Water Quality and Conservation of the Pearl River Delta, Ministry of Education, Guangzhou University, Guangzhou 510006, China

[b]Key Laboratory of Drinking Water Science and Technology, Research Center for Eco-Environmental Sciences, Chinese Academy of Sciences, Beijing 100085, China

[*]Corresponding author

Phone: +86-20-39346609

E-mail: huchun@rcees.ac.cn / huchun@gzhu.edu.cn

The Supporting Information included:

5 Texts

4 Tables

11 Figures

25 Pages

Text S1:

Chemicals. Cobalt nitrate hexahydrate ($Co(NO_3)_2•6H_2O$), zinc nitrate hexahydrate ($Zn(NO_3)_2•6H_2O$), 2-methylimidazole, potassium monopersulfate triple salt ($KHSO_5•1/2KHSO_4•1/2K_2SO_4$, PMS), methanol, ethanol, bisphenol A (BPA), 2-chlorophenol (2-CP), 2,4-dichlorophenoxyacetic acid (2,4-D), diphenhydramine (DP), benzoquinone (BQ), 5,5-dimethyl-1-pyrroline N-oxide (DMPO), 2,2,6,6-tetramethyl-4-piperidinol (TMP) were obtained from Adamas Reagent Co., Ltd. Ciprofloxacin (CIP) and *tert*-butyl alcohol (TBA) were purchased from TCI (Shanghai) Chemical Industry Development Co., Ltd and Aladdin Industrial Corporation, respectively. The above reagents are commercially available analytical pure and were directly used without further purification. The molecular structures of various organic pollutants are shown in **Figure S1**. Ultrapure water was used in all the experiments.

Text S2:

Synthesis Procedures. The ZIF-8 was first synthesized as the crystal seed using a co-precipitation method. $Zn(NO_3)_2•6H_2O$ (0.04 M) was dissolved in 150 mL methanol to form solution 1, meanwhile 0.15 M 2-methylimidazole was dissolved in 150 mL methanol to form solution 2. Subsequently, solution 1 and solution 2 were mixed together and stirred at room temperature for 24 h. Then the white precipitants were centrifuged and rinsed with methanol for three times and dried at 60 ℃ prior to use. For the preparation of ZIF-8@ZIF-67, $Co(NO_3)_2•6H_2O$ (0.04 M) was firstly dissolved in 150 mL methanol to form solution 3, and then a certain amount of ZIF-8 was dispersed in 150 mL methanol, followed by the addition of solution 3 and solution 2 in

sequence. After being mixed and stirred for 24 h, the light purple precipitates were centrifuged, washed by methanol for three times, and dried at 60 ℃. The light purple solids were then subjected to pyrolysis in a tube furnace at 920 ℃ for 3 h under Ar atmosphere. After cooling naturally, the black powders were collected and washed in 3 M H_2SO_4 solution under stirring for 24 h to finally obtain the NCoHCP product.

Text S3:

Characterizations. Powder X-ray diffraction patterns were obtained by a Bruker D8 Advance diffractormeter with Cu Kα radiation (λ = 1.54178 Å). The morphology and microstructure were observed on a FEI Quanta FEG 250 scanning electron microscopy (SEM) and a FEI Tecnai G2 F20 transmission electron microscopy (TEM). The distribution of elements in the sample was examined using energy dispersive spectroscopy (EDS) attached to the SEM and TEM. The specific surface area and pore volume were determined via N_2 adsorption-desorption measurements at 77 K on a Micrometrics ASAP 2460 apparatus. Raman spectra were recorded on a LabRAM HR Evolution (HORIBA, France) equipped with a CCD detector using a laser source at an excitation line of 532 nm. X-ray photoelectron spectroscopy (XPS) data were acquired on a Thermo ESCALAB 250 Xi instrument using monochromatic Al Kα radiation. The cobalt amount of the catalyst was measured by inductively coupled plasma optical emission spectrometry (ICP-OES) (NexION 2000, PerkinElmer). X-ray Absorption Spectroscopy (XAS) was performed at the beamline BL14W1 of Shanghai Synchrotron Radiation Facility (SSRF), in China. Extended X-ray Absorption Fine Structure (EXAFS) data were collected through a fixed-exit double-crystal Si (111)

monochromator. The acquired EXAFS data were processed according to the standard procedures using the ATHENA module implemented in the IFEFFIT software packages.[1]

Text S4:

Experimental Procedures and Analyses. Catalytic oxidation of bisphenol A (BPA) over NCoHCP via PMS activation was carried out in a 100 mL beaker with BPA solution (30 mL, 0.1 mM), PMS (4 mM) and catalyst (0.2 g L^{-1}) in a constant temperature controlled water bath at 30 ℃. As the reaction proceeded, 1 mL aliquots of reaction solution were withdrawn by syringe at designated time intervals, and immediately filtered through a Millipore filter (0.22 μm) for analysis. The degradation of organic pollutants was monitored by a 1260 Infinity HPLC (Agilent, USA) equipped with a UV detector and a Poroshell 120 EC-C18 column (4.6 × 100 mm, 2.7 μm). The mobile phases and detection wavelengths for various organic contaminants are displayed in **Table S1**. The flowing rate of mobile phase was set as 1 mL min^{-1}. The removal efficiency was calculated by the following equation.

$$\text{Removal efficiency (\%)} = 100 \times (C_0 - C_t)/C_0 \quad (1)$$

where C_0 and C_t are the initial organic pollutant concentration and the concentration at a reaction time t during the catalytic reaction, respectively.

The amount of metal ions leaching from the catalyst after catalytic reaction was measured using inductively coupled plasma mass spectrometry (ICP-MS) (NexION 300, PerkinElmer). The stability of NCoHCP was assessed by cycling tests. The PMS concentration remaining in the solution was determined according to the previous work

with some modification.[2] Briefly, a high-concentration solution of iodide (KI, 0.5 M) with bicarbonate buffer ($NaHCO_3$, 0.05 M) was prepared first, and then 0.1 mL filtered sample was mixed with the above iodide solution (4.9 mL). After reaction for 20 min, the chromogenic sample was detected at λ = 352 nm.

The electron paramagnetic resonance (EPR) measurements for in situ detection of hydroxyl radical ($^{\bullet}OH$)/sulfate radical ($SO_4^{\bullet-}$) and superoxide radical ($O_2^{\bullet-}$) were conducted on a Bruker A300 spectrometer at room temperature using 5,5-dimethyl-1-pyrroline N-oxide (DMPO) as the spin trapping agent in the aqueous and methanol media, respectively. Singlet oxygen ($^1O_2$) was detected by EPR spectrometry with the spin-trapping agent of 2,2,6,6-tetramethyl-4-piperidinol (TMP) in aqueous solution. Quenching experiments were performed to discern the reactive oxygen species (ROS) generated in the catalytic systems with *tert*-butyl alcohol (TBA), ethanol, benzoquinone (BQ) and β-carotene as chemical scavengers for $^{\bullet}OH$, $SO_4^{\bullet-}$, $O_2^{\bullet-}$ and $^1O_2$, respectively. Each experiment was carried out in triplicates and the average data with the standard deviations were presented.

Text S5:

Theoretical Computations. All the calculations were conducted based on the density functional theory (DFT) calculations using Vienna *ab initio* simulation package (VASP) code with the standard frozen-core projector augmented-wave (PAW) method.[3] The generalized gradient approximation (GGA) of Perdew-Burke-Ernzerh (PBE) function[4] was employed for exchange-correlation potential. The cut-off energy was 400 eV and atoms were fully relaxed until the Hellmann-Feynman forces were less than 0.02 eV

$Å^{-1}$. The effect of van der Waals interactions was considered by using the empirical correction method proposed by Grimme (DFT-D3) with the Becke and Johnson (BJ)-damped. Bader charge analysis was performed to calculate the effective charge for the NCoHCP catalyst before and after PMS adsorption. A *k*-mesh of $2 \times 2 \times 1$ was used for the sampling of the first Brillouin-zone.

Table S1. Parameters for measurement of various organic pollutants by HPLC.

Organic pollutant	Mobile phase	Detection wavelength (nm)
Bisphenol A (BPA)	methanol/water (70:30, v/v)	225
2-chlorophenol (2-CP)	methanol/water (60:40, v/v)	275
2,4-dichlorophenoxyacetic acid (2,4-D)	acetonitrile/water (0.08% phosphoric acid) (20:80, v/v)	278
Ciprofloxacin (CIP)	acetonitrile/water (0.08% phosphoric acid) (60:40, v/v)	220
diphenhydramine (DP)	acetonitrile/water (0.08% phosphoric acid) (50:50, v/v)	221

Table S2. EXAFS data fitting results from Co K-edge of NCoHCP.

Sample	Path	*N*	*R* (Å)	σ^2 (Å^2)	ΔE_0 (eV)	*R*-factor
NCoHCP	Co–Co	5.32	2.49	0.006	5.79	0.003
	Co–N	0.99	1.92			

N is coordination number, *R* is the distance between absorber and backscatter atoms, σ^2 is Debye-Waller factor to account for both thermal and structural disorders, ΔE_0 is inner potential correction; *R* factor indicates the goodness of the fit.

Table S3. The catalytic performance comparison of recently reported catalysts for PMS activation. The specific activity was obtained by rate constant normalized to BET surface area (S_{BET}) and loading of a catalyst.

Catalyst (loading, g L^{-1})	S_{BET} (m^2 g^{-1})	Pollutant (mg L^{-1})	PMS (g L^{-1})	PMS decomposition	Removal efficiency	Rate constant (min^{-1})	Specific activity (L min^{-1} m^{-2})	Ref.
CPPy-F-8 (0.1)	74.9	Phenol (20)	1.0	19% (120 min)	97% (120 min)	0.03	0.004	[5]
NG (0.2)	99.3	Phenol (20)	2.0	–	100% (90 min)	0.071	0.003	[6]
$CuFe_2O_4$-Fe_2O_3 (0.2)	63.0	BPA (5)	0.36	10% (10 min)	100% (10 min)	0.14	0.011	[7]
NCNTFs (0.05)	410.0	BPA (25)	0.4	–	97% (30 min)	0.216	0.010	[8]
NoCNT-700 (0.1)	450.0	Phenol (20)	2.0	–	100% (20 min)	0.247	0.005	[9]
Fe^{3+}-g-C_3N_4 (0.1)	51.7	4-CP (13)	0.3	–	100% (15 min)	0.254	0.049	[10]
FeMn-350 (0.5)	23.5	BPA (80)	0.2	70% (60 min)	100% (30)	0.295	0.025	[11]
NG-700 (0.1)	227.5	Phenol (20)	2.0	–	100% (30 min)	0.319	0.014	[12]

NC-900 (0.2)	331.99	BPA (23)	0.6	–	90% (5 min)	0.46	0.007	[13]
$Fe_1Mn_5Co_4$-N@C (0.1)	66.0	BPA (20)	0.2	–	100% (10 min)	0.48	0.072	[14]
NGC-700 (0.1)	1236.0	BPA (20)	0.2	–	100% (6 min)	1.05	0.008	[15]
FeCo-NC (0.1)	375.0	BPA (20)	0.2	–	100% (4 min)	1.252	0.033	[16]
NCN-900 (0.1)	1218.7	BPA (23)	0.6	48% (2 min)	100% (2 min)	3.10	0.025	[17]
NCoHCP (0.2)	302.9	BPA (23)	1.2	45% (1 min)	100% (45 s)	7.80	0.129	This work

Table S4. Water quality parameters of actual industrial wastewater sample.

Parameters	
pH	7.78
Conductivity (μS cm^{-1})	105.42
TOC (mg L^{-1})	36.99
BOD_5 (mg L^{-1})	15.00
COD (mg L^{-1})	110.32
Mn (mg L^{-1})	0.007
Fe (mg L^{-1})	0.058
Co (mg L^{-1})	0.008
Cu (mg L^{-1})	0.141
Ni (mg L^{-1})	0.020
Zn (mg L^{-1})	0.057

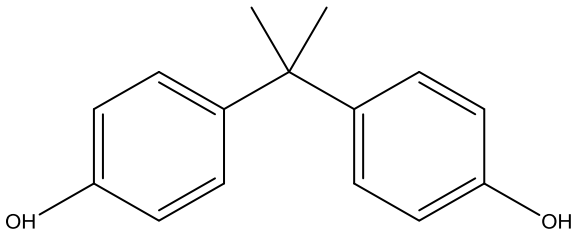

Bisphenol A (BPA)

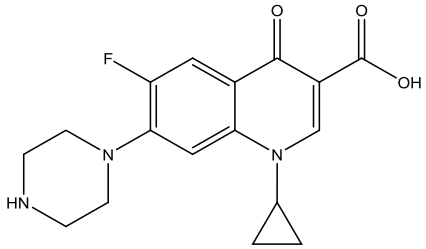

Ciprofloxacin (CIP)

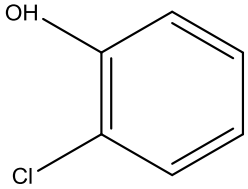

2-chlorophenol (2-CP)

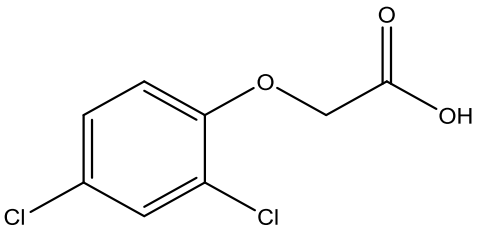

2,4-dichlorophenoxyacetic acid (2,4-D)

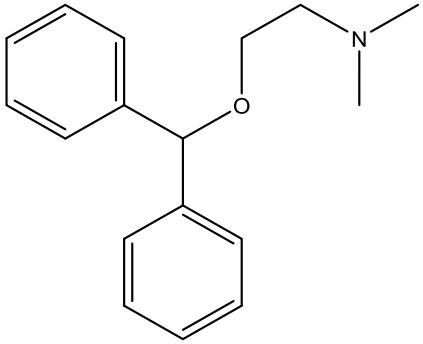

Diphenhydramine (DP)

Figure S1. Molecular structures of various organic pollutants.

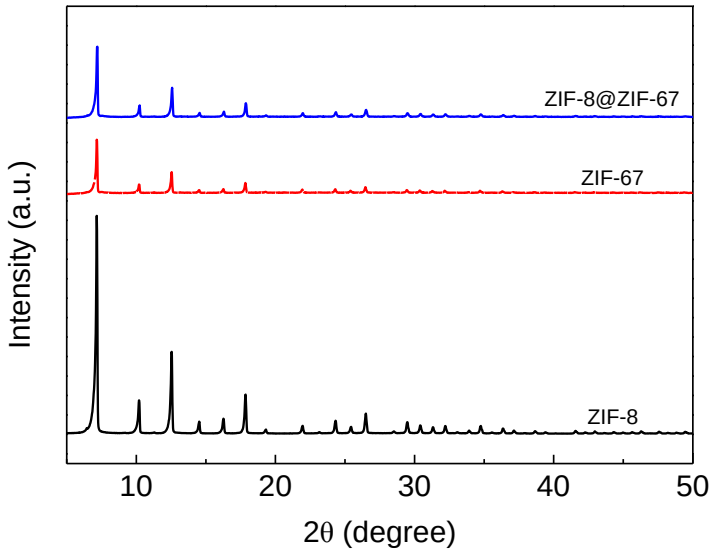

Figure S2. XRD patterns of ZIF-8, ZIF-67, and ZIF-8@ZIF67.

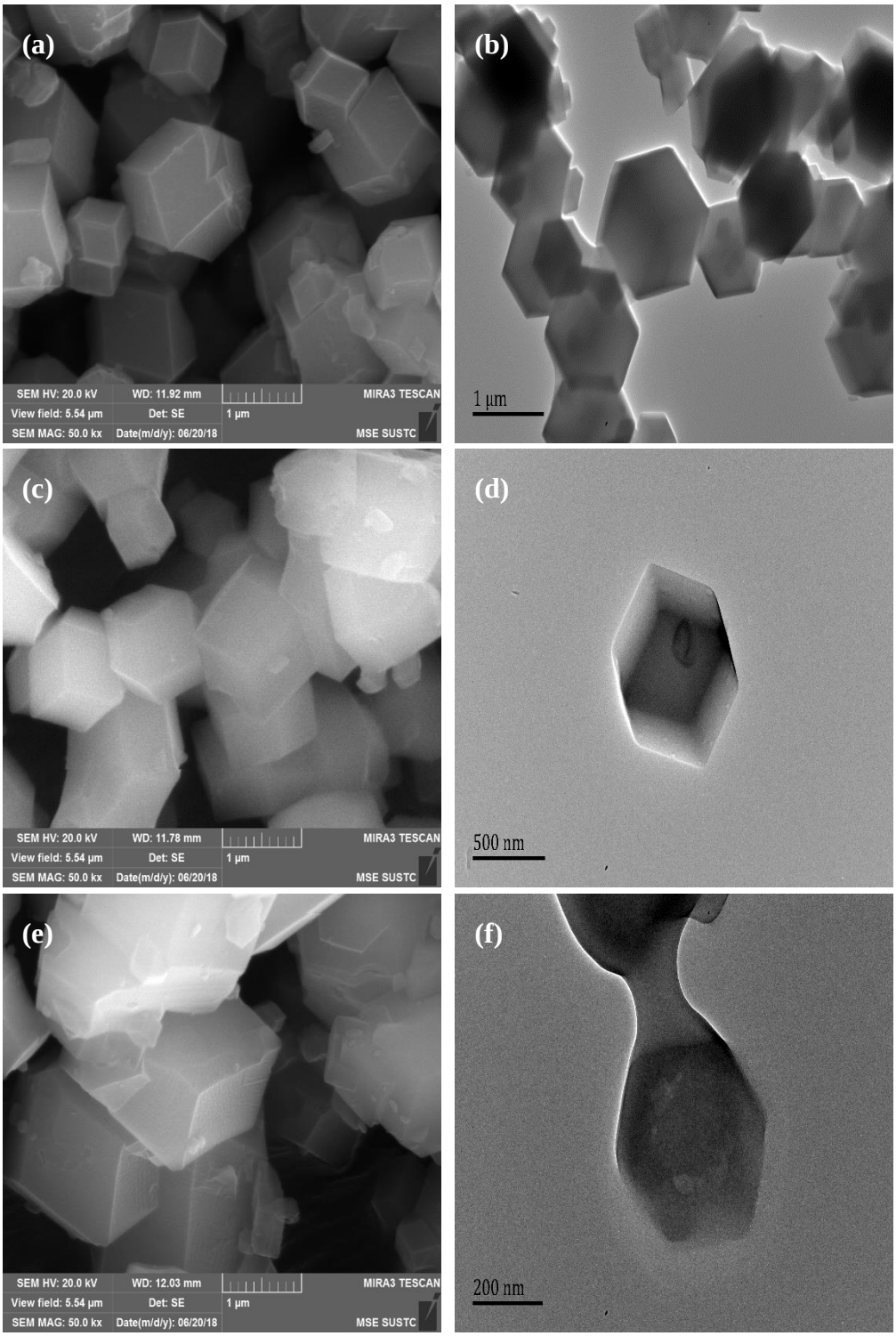

Figure S3. SEM images of (a) ZIF-8, (c) ZIF-67, and (e) ZIF-8@ZIF-67. TEM images of (b) ZIF-8, (d) ZIF-67, and (f) ZIF-8@ZIF-67.

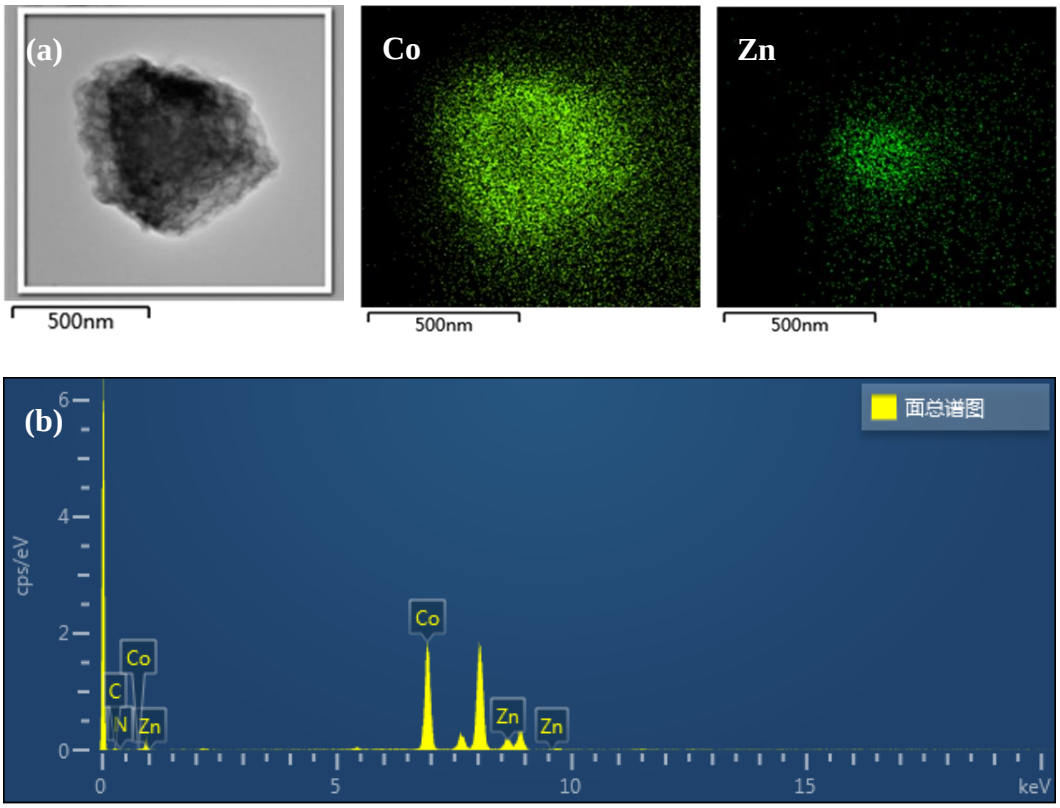

Figure S4. TEM and EDS elemental mapping images of ZIF-8@ZIF-67.

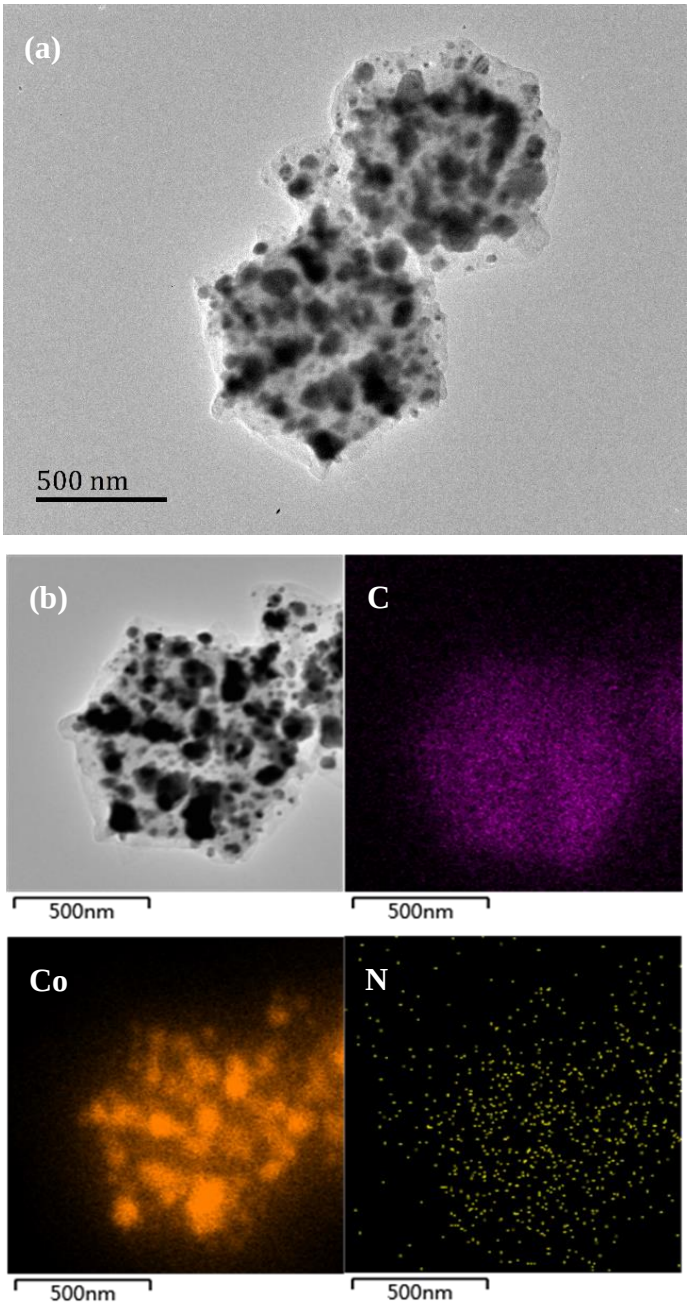

Figure S5. (a) TEM image and (b) corresponding elemental mapping of C, Co, and N for Co-NC (annealed ZIF-67).

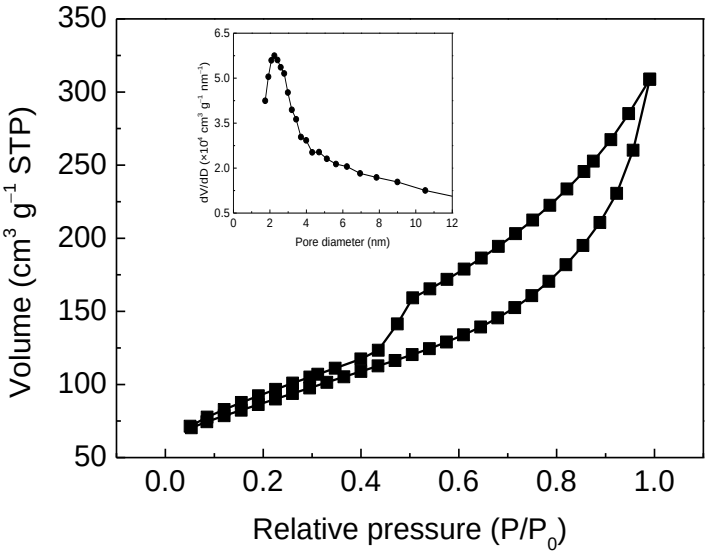

Figure S6. N_2 adsorption-desorption isotherm curve for NCoHCP.

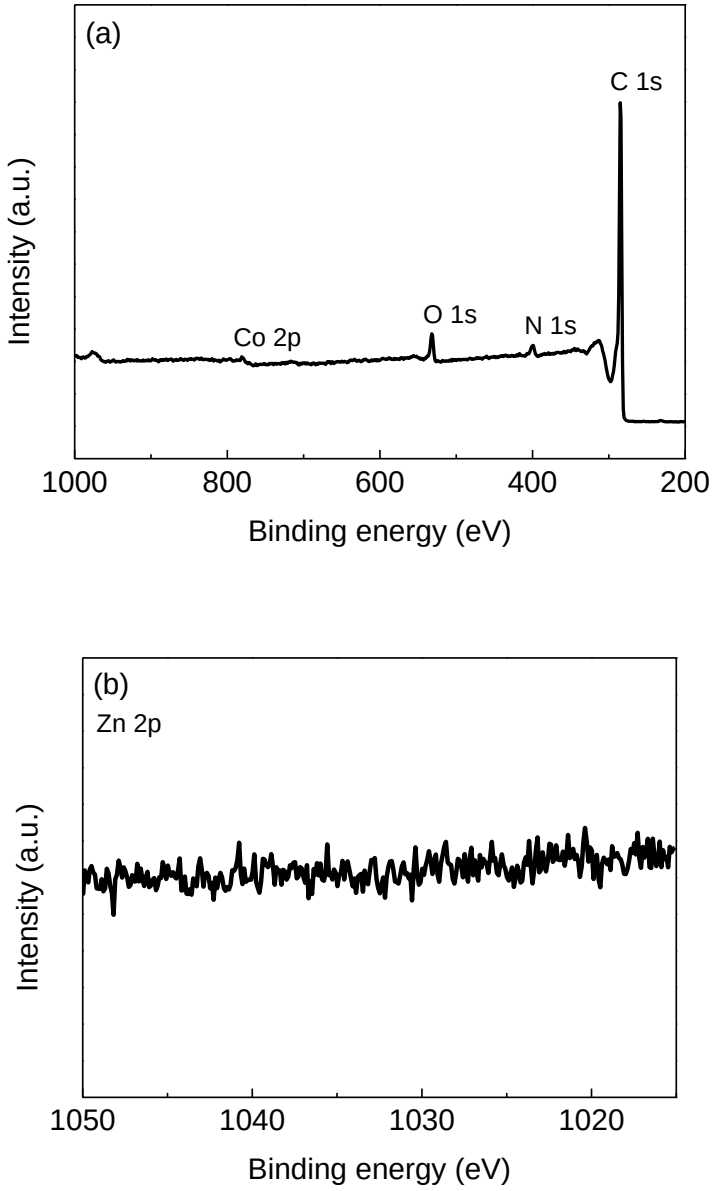

Figure S7. (a) XPS survey and (b) high-resolution XPS Zn 2p spectrum of NCoHCP.

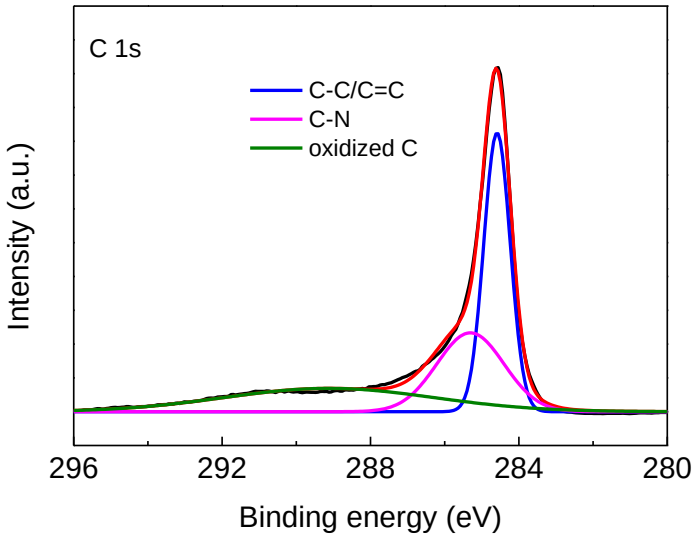

Figure S8. High-resolution XPS spectrum of C 1s for NCoHCP.

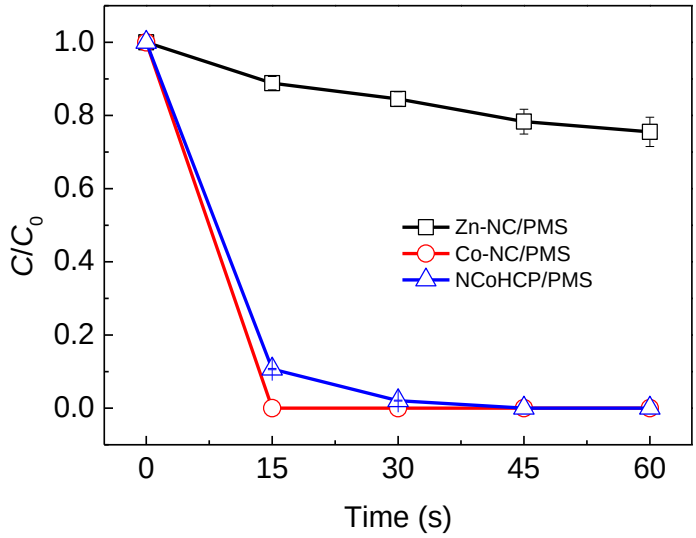

Figure S9. Catalytic activity of Zn-NC (annealed ZIF-8) and Co-NC (annealed ZIF-67) for PMS activation. Reaction conditions: [BPA] = 0.1 mM; [catalyst] = 0.2 g L^{-1}; [PMS] = 4 mM; [Temp] = 30 ℃; initial pH = 6.7.

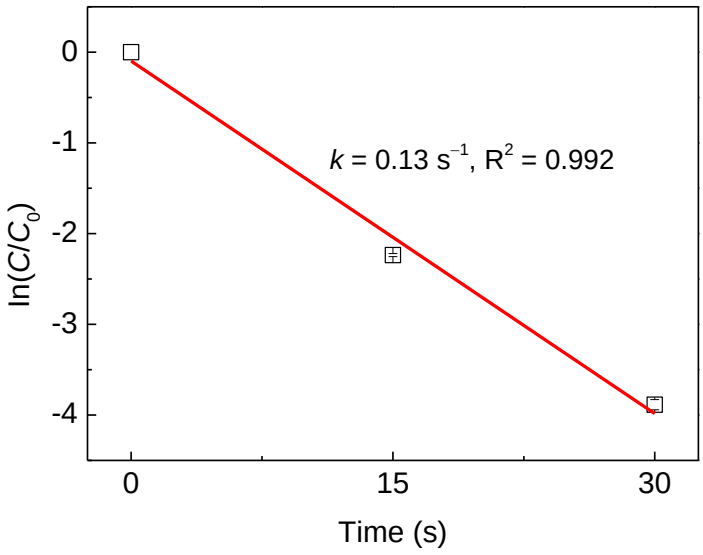

Figure S10. Pseudo-first-order kinetic model of BPA oxidation over NCoHCP via PMS activation. Reaction conditions: [BPA] = 0.1 mM; [NCoHCP] = 0.2 g L^{-1}; [PMS] = 4 mM; [Temp] = 30 ℃; initial pH = 6.7.

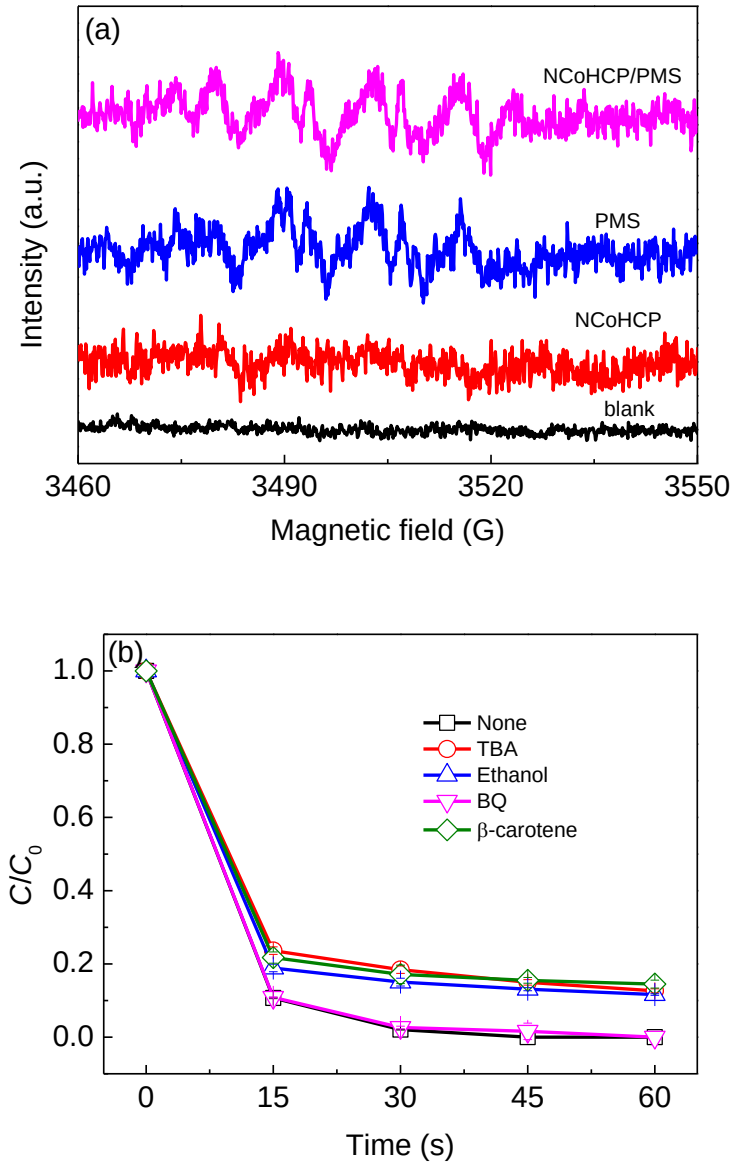

Figure S11. (a) EPR spectra for $O_2^{\bullet-}$ of various systems. (b) Catalytic oxidation of BPA in the NCoHCP/PMS system in the presence of different scavengers. Reaction conditions: [BPA] = 0.1 mM; [NCoHCP] = 0.2 g L^{-1}; [PMS] = 4 mM; [Temp] = 30 ℃; [TBA] = [Ethanol] = 1 M (if needed); [BQ] = 10 mM (if needed); [β-carotene] = 0.1 mM (if needed); initial pH = 6.7 (if needed).

References

(1) Yu H. S.; Wei. X.J., Li, J.; Gu, S. Q.; Zhang, S.; Wang, L. H.; Ma, J. Y.; Li, L. N.; Gao, Q.; Si, R.; Sun, F. F.; Wang, Y.; Song, F.; Xu, H. J; Yu, X. H.; Zou, Y.; Wang, J. Q.; Jiang, Z.; Huang, Y. Y. The XAFS beamline of SSRF. *Nucl. Sci. Tech.* **2015,** *26*, 50102-50104.

(2) Liang, C.; Huang, C. F.; Mohanty, N.; Kurakalva, R. M. A rapid spectrophotometric determination of persulfate anion in ISCO. *Chemosphere* **2008,** *73*, 1540-1543.

(3) Kresse, G.; Furthmuller, J. Efficient iterative schemes for ab initio total-energy calculations using a plane-wave basis set. *Phys. Rev. B* **1996**, *54*, 169-186.

(4) Perdew, J. P.; Burke, K.; Ernzerhof, M. Generalized gradient approximation made simple. *Phys. Rev. Lett.* **1996**, *77*, 3865-3868.

(5) Hu, P.; Su, H.; Chen, Z.; Yu, C.; Li, Q.; Zhou, B.; Alvarez, P. J. J.; Long, M. Selective degradation of organic pollutants using an efficient metal-free catalyst derived from carbonized polypyrrole via peroxymonosulfate activation. *Environ. Sci. Technol.* **2017**, 51, 11288-11296.

(6) Wang, C.; Kang, J.; Sun, H.; Ang, M.; Tadé, M.; Wang, S. One-pot synthesis of N-doped graphene for metal-free advanced oxidation processes. *Carbon* **2016**, 102, 279-287.

(7) Oh, W. D.; Dong, Z.; Hu, Z. T.; Lim, T. T., A novel quasi-cubic $CuFe_2O_4$-Fe_2O_3 catalyst prepared at low temperature for enhanced oxidation of bisphenol A via peroxymonosulfate activation. *J. Mater. Chem. A* **2015**, 3, 22208-22217.

(8) Ma, W.; Wang, N.; Fan, Y.; Tong, T.; Han, X.; Du, Y. Non-radical-dominated catalytic degradation of bisphenol A by ZIF-67 derived nitrogen-doped carbon nanotubes frameworks in the presence of peroxymonosulfate. *Chem. Eng. J.* **2018**. 336, 721-731.

(9) Duan, X.; Sun, H.; Wang, Y.; Kang, J.; Wang, S., N-doping-induced nonradical reaction on single-walled carbon nanotubes for catalytic phenol oxidation. *ACS Catal.* **2015**, 5, 553-559.

(10) Li, H.; Shan, C.; Pan, B. Fe(III)-doped g-C_3N_4 mediated peroxymonosulfate activation for selective degradation of phenolic compounds via high-valent iron-oxo species. *Environ. Sci. Technol.* **2018**, 52, 2197-2205.

(11) Yu, L.; Zhang, G.; Liu, C.; Lan, H.; Liu, H.; Qu, J. Interface stabilization of undercoordinated iron centers on manganese oxides for nature-inspired peroxide activation. *ACS Catal.* **2018**, 8, 1090-1096.

(12) Duan, X.; Ao, Z.; Sun, H.; Indrawirawan, S.; Wang, Y.; Kang, J.; Liang, F.; Zhu, Z.; Wang, S. Nitrogen-doped graphene for generation and evolution of reactive radicals by metal-free catalysis. *ACS Appl. Mater. Interfaces* **2015**, 7, 4169-4178.

(13) Gao, Y.; Zhu, Y.; Chen, Z.; Zeng, Q.; Hu, C. Insights into the difference in metal-free activation of peroxymonosulfate and peroxydisulfate. *Chem. Eng. J.* **2020**, 394, 123936-123946.

(14) Li, X.; Ao, Z.; Liu, J.; Sun, H.; Rykov, A. I.; Wang, J. Topotactic transformation of metal-organic frameworks to graphene-encapsulated transition-metal nitrides as efficient Fenton-like catalysts. *ACS Nano* **2016**, 10, 11532-11540.

(15) Luo, R.; Li, M.; Wang, C.; Zhang, M.; Nasir Khan, M. A.; Sun, X.; Shen, J.; Han, W.; Wang, L.; Li, J. Singlet oxygen-dominated non-radical oxidation process for efficient degradation of bisphenol A under high salinity condition. *Water Res.* **2019**, 148, 416-424.

(16) Li, X.; Huang, X.; Xi, S.; Miao, S.; Ding, J.; Cai, W.; Liu, S.; Yang, X.; Yang, H.; Gao, J.; Wang, J.; Huang, Y.; Zhang, T.; Liu, B. Single cobalt atoms anchored on porous N-doped graphene with dual reaction sites for efficient Fenton-like catalysis. *J. Am. Chem. Soc.* **2018**, 140, 12469-12475.

(17) Gao, Y.; Chen, Z.; Zhu, Y.; Li, T.; Hu, C. New insights into the generation of singlet oxygen in the metal-free peroxymonosulfate activation process: Important role of electron-deficient carbon atoms. *Environ. Sci. Technol.* **2019**, 54, 1232-1241.